Defence Research and Development Canada
Recherche et développement pour la défense Canada

CAN UNCLASSIFIED

DRDC | RDDC
technologysciencetechnologie

Simulation of Radar Detection and Target Tracking Against Electronic Counter Measures (ECM) Using Adaptive Multifunction Radar (Adapt_MFR) v3.2.14—Final Contract Report

Bing Yue
C-CORE

Prepared by:
C-CORE
4043 Carling Ave., Suite 202
Ottawa (Ontario) K2K 2A4
Canada

PSPC Contract Number: W7714-176210/001/IPS
Technical Authority: Jack Zhen Ding, Defence Scientist
Contractor's date of publication: June 2018

Defence Research and Development Canada

Contract Report
DRDC-RDDC-2018-C163
November 2018

CAN UNCLASSIFIED

Canada

IMPORTANT INFORMATIVE STATEMENTS

Abstract

This report summarizes the work done under Task 2 of contract W7714-176210/001/IPS. This work includes design and implementation of Electronic Counter Measures (ECM) techniques for the Adaptive Multi-Function Radar (Adpat_MFR) simulator and evaluation of Adapt_MFR's detection and tracking performance against ECMs given different system setups including single or multiple radar scenarios, varied false alarm rates (FA), tracker gate size, and beam scheduling technique. The implemented ECMs include range gate pull off (RGPO) on the target, and standoff jamming broadcasting narrow-band noise or white noise covering a specified bandwidth. The existing FA routine in Adapt_MFR has also been modified by adding FAs to the system on all scans, including detection scans.

This page intentionally left blank.

Table of contents

List of figures

List of tables

This page intentionally left blank.

1 Introduction

Defence Research and Development Canada Ottawa (DRDC Ottawa) has contracted C-CORE with contract W7714-176210/001/IPS, to provide Programmer/Analyst support services to generate simulated radar data and to process and analyze radar data that has been generated through simulation or experimental trials. As part of this “as and when requested ”contract, C-CORE has undertaken Task 2, which focuses on implementing and evaluating various maneuvering scenarios in the radar simulation tool Adaptive Multi-Function Radar (Adapt_MFR) simulator. The work has involved verifying and implementing new functionality with the simulation environment, including Electronic Counter-Measure (ECM) techniques, as well as implementing and troubleshooting the false alarm (FA) routine to allow adaptive tracking performance evaluation. The work has taken place between July 2017 and June 2018.

This document contains a detailed overview of the work and results from this task. Section 2 describes the implementation of ECM techniques and testing results as well as the modification and verification of the existing FA routine. In Section 3, scenarios have been designed to investigate various radar system operation parameters against ECM including single and multiple radar networks, adaptive and non-adaptive scheduling techniques, different gate sizes, and with different FA settings.

2 ECM technique Development and Implementation

Ever since radar has been used for air target detection and tracking to gain superior situation awareness in combat and other scenarios, ECM techniques have been designed and developed to confuse, overwhelm or mislead adversary radar sensors so that they are unable to detect, track or attack critical assets under protection. Radar detection and tracking against ECMs is an ongoing challenge for naval radar operations.

The focus of one of the work sub-packages has thus been to implement ECM capabilities in Adapt_MFR to better understand their impacts on highly maneuvering target detection and tracking using marine radars. The implemented ECM techniques in this task includes range gate pull off (RGPO) on the target and standoff jammers broadcasting narrow-band or a defined noise bandwidth. In addition, the FA routine in previous versions of Adapt_MFR was found to only model FAs on tracking and confirmation beams, this routine has thus been modified to allow FAs to be included on all radar beams.

The design, implementation and testing of the FA fix, jamming, and RGPO functions will be described in the following sub-sections.

2.1 False Alarm Function

To evaluate tracking metrics and performance the Adapt_MFR FA routine was examined to ensure proper functionality. The FA routine was found to only enable FAs on tracking and confirmation beams, modifications were required to fix this issue and to confirm that the fix did not affect any other routines, such as time-balancing or scheduling. This section will outline the current implementation of the FA routine, and then show results that confirm proper functionality based on user input parameters, and time-balancing and scheduling functionality.

2.1.1 Implementation

Adapt_MFR provides a FA environment that is based on a probability of false alarm (PFA) occuring in any given radar range cell. This probability is used by the simulation tool to generate FAs within each simulated beam during a simulation. This feature has to be enabled from the *General Parameter Menu* (see Figure 1).

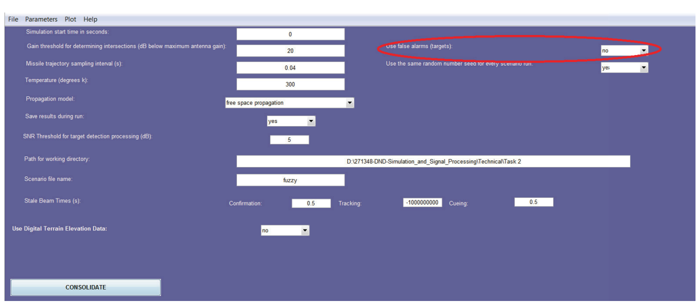

Figure 1: *Adapt_MFR General Parameter page, showing the FA toggle*

The PFA can now be modified for detection, track and confirmation beams by changing the value in the *Radar and Processing/waveform* menu (see Figure 2).

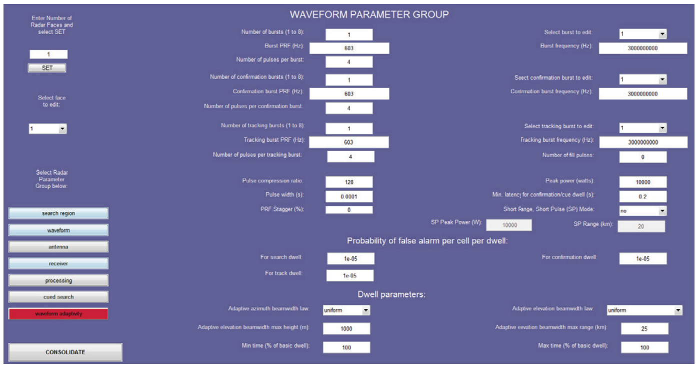

Figure 2: *Adapt_MFR Radar and Processing - waveform page, showing PFA values*

These values are used to calculate the probability of a FA on each scan using statistical permutation and combination rules. The scan probability is dependent on both the unambiguous range R_{unamb} and range resolution Δr given by:

$$R_{unamb} = \frac{c}{2PRF} \tag{1}$$

$$\Delta r = \frac{cPW}{2C_p} \tag{2}$$

where:

c is the speed of light (m/s), PRF is the scan pulse repetition frequency (Hz), PW is the pulsewidth (s), and Cp is the pulse-compression ratio.

The scan probability PFA_{scan} is then given by:

$$PFA_{scan} = \frac{R_{unamb}}{\Delta r} PFA(1-PFA)^{\left(\frac{R_{unamb}}{\Delta r}-1\right)} \tag{3}$$

and is then used to schedule a FA after each beam scan during a radar simulation.

At the start of Task 2, this value was only used on *confirmation* or *tracking* beams, thus the true FA probability was much less than the value entered by the user. To fix this, the *add_false_alarms* function was modified to ensure that FAs were added during detection beams as well.

In addition to enabling FAs during detection beams, the FA routine solves for FA positions within the radar waveform specifications. The current implementation of this FA position check ensures that the FA falls outside of the radar blind range r_{min} and the first ambiguous range bin r_{max}. These are defined as:

$$r_{min} = \frac{cPW}{2} \tag{4}$$

$$r_{max} = \frac{c}{2PRF} \tag{5}$$

2.1.2 Testing

The parameters for testing these changes to the FA implementation are listed in the Adapt_MFR GUI in Figure 2. For these values, the blind range is 15km and the ambiguous range is slightly less than 249km. These parameters yield the following PFA_{scan} rate for each of set PFA rates.

Description	PFA	PFA_{scan}
single missile scenario	0	0
single missile scenario	0.0001	0.1717
single missile scenario	0.00001	0.0208

2.2 Jamming Function

Jamming techniques are a kind of active ECM techniques, where the standoff jammer transmits an interference noise signal in the adversary radar direction so that the actual target refection is completely or partially submerged by interference. The primary advantage of noise jamming is that only minimal details about the enemy equipment need be known [1].

2.2.1 Implementation

Two types of jamming techniques were implemented in previous versions of Adapt_MFR: spot and barrage jamming. A spot jammer (or narrow-band jammer), can generate power concentrated in a very narrow bandwidth or identical to the frequency of the adversary radar. A barrage jammer is similar, but is capable of spreading its output power over a certain bandwidth much wider than that of the radar signal. However, both jamming functions implemented in the previous versions had critical limitation: the position of the jammer was fixed during the simulation. This severely constrains the jamming impact in the simulations. The modified jamming routine allows users to define jammer trajectories. Figure 3 and Figure 4 show the old and new Jammer GUI respectively. The parameters used to define a jammer are summarized in Table 1. These parameters are saved in a new data structure *jammer* in the parameter file **.mfr* used by Adapt_MFR.

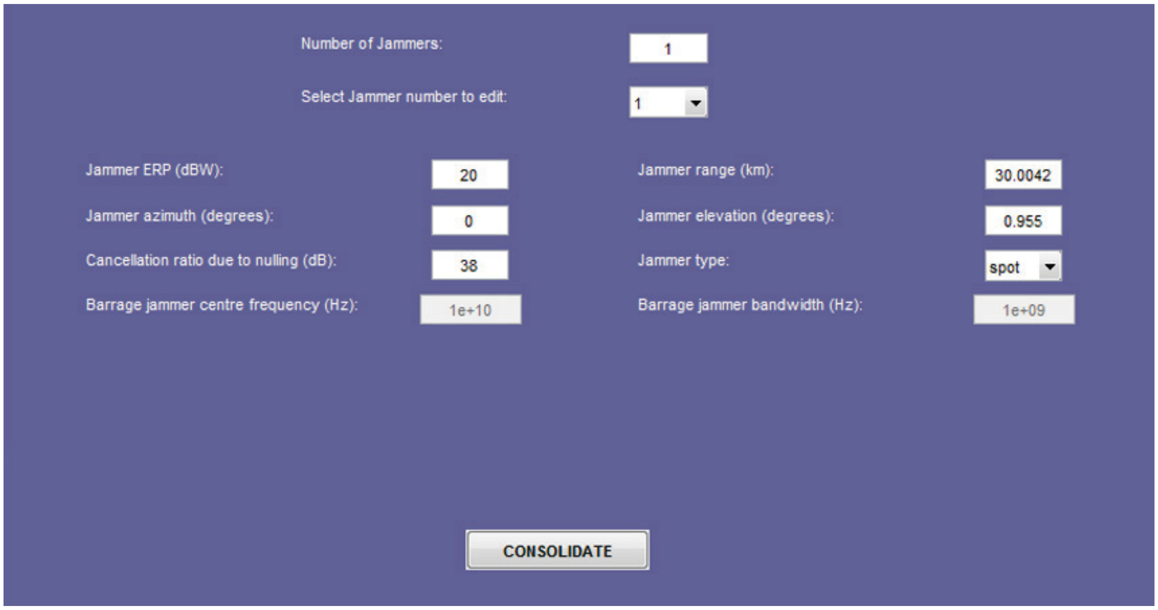

Figure 3: *Jammer parameter GUI before Adapt_MFR v3.2.14*

Figure 4: *Jammer parameter GUI in Adapt_MFR v3.2.14*

Figure 5 displays a jammer trajectory defined using the parameters in Table 1. The jammer has an speed of 168 m/s counterclockwise and flies on an altitude of 3050 m, its race-course pattern trajectory includes 4 legs with 180 seconds total flying time.

Table 1: *Input parameters for jammer function*

Number of standoff Jammers:	1			
Jammer start time:	0			
Jammer ERP (dBW):	20			
Jammer type:	spot			
Cancellation ration due to nulling (db):	38			
Initial azimuth position (degree):	45			
Initial ground range from radar (km):	100			
Initial altitude (m):	20			
Initial forward speed (m/s):	168			
Initial heading (0 degree towards target):	-45			
Number of legs in trajectory:	4			
	Leg1	Leg2	Leg3	Leg4
Duration of leg thrust (s):	40	50	40	50
Speed at end of leg (m/s):	168			
Altitude at end of leg (m):	3050			
Jammer heading at end of leg (degree):	0	180	0	180

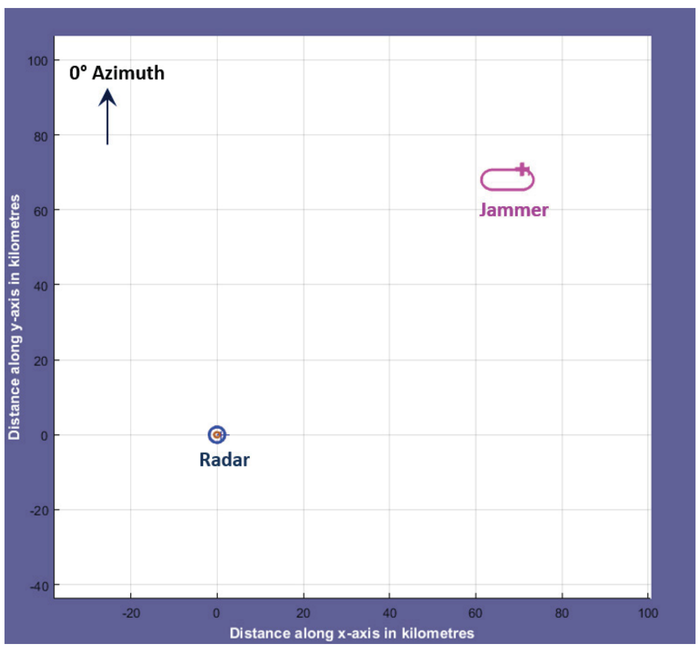

Figure 5: *Jammer trajectory defined using parameters in Table 1*

Table 2 lists the modified and new jamming functions in Adapt_MFR v3.2.14.

Table 2: Modified and new jamming Functions in Adapt_MFR v3.2.14

Functions Modified:	
adaptmfr_run.m	*Main*
detSNR.m	*Main*
radRng3.m	*Main*
compute_radaRangeEquation.m	*Main*
doppler_mfr.m	*Main*
surfMfr4Mod_dted.m	*Main*
surfMfr4Mod_opt.m	*Main*
anomPrp3.m	*Main*
adapt_mfr.m	*GUI*
cbConsolidate.m	*GUI*
cbLoadParams.m	*GUI*
cbPlaneView.m	*GUI*
cbSaveParms.m	*GUI*
editUiControl.m	*GUI*
cbJammerParams.m	*GUI*
saveJamParams.m	*GUI*
New Functions:	
get_jammer_position.m	*Main*
init_jammer_trajectory.m	*Main*
changeJammerLegs.m	*GUI*

2.2.2 Testing

Two scenarios, S1 and S2, were designed to test the new jamming routine, each scenario includes three sub-scenario. The trajectories of the target and jammer in each sub-scenario are displayed in Figure 6, with S1 displayed on the left column and S2 on the right. The radar was at the same location (0,0) and the target always flew the same trajectory in each sub-scenario. The jammer flying area was changed for each sub-scenario to investigate jammer impact on the target given different distance between them. The target flew at a constant speed (200 m/s) along an 12 km long X-direction trajectory, at an altitude of 500 m and 20 km away from the radar in the Y-direction. The jammer flew the same trajectory (clockwise) with a constant speed (168m/s) though it started at a different position for each sub-scenario. The target and jammer in each sub-scenario had the same trajectory time of 120 seconds.

In sub-scenario S1_A and S2_A, the jammer started at 0° in azimuth with 21 km and 30 km ground range from the radar respectively. In sub-scenario S1_B and S2_B, the jammer started at the same Y locations as in sub-scenario As but offset by 5 km and 7 km in the X-direction respectively; sub-scenario C combined the jammer in sub-scenariuo A and B.

The target track estimation result for each sub-scenario was displayed in Figure 7. One can see that the radar's target tracking was interrupted by the jammer in all cases but for different lengths of time. Comparing the tracking results in each row, the jammer in S1 sub-scenario (left) caused more track loss compared to the jammer in S2 sub-scenario (right), where the difference between each pair on the same row (S1_A and S2_A, S1_B and S2_B, and S1_C and S2_C) is the distance between the jammer and target, they are closer in S1 sub-scenario on the left.

From this experiment, one can see that the distance between the jammer and target is a critical factor in the target's visibility to the radar. Another observation from Figure 7 is the linear superposition effect on target's tracking result when multiple jammers are used. One can see that the tracking result from sub-scenario C is the combined result of sub-scenario A and B, i.e. the impact of multiple jammers on target tracking is the contribution from all individual jammers.

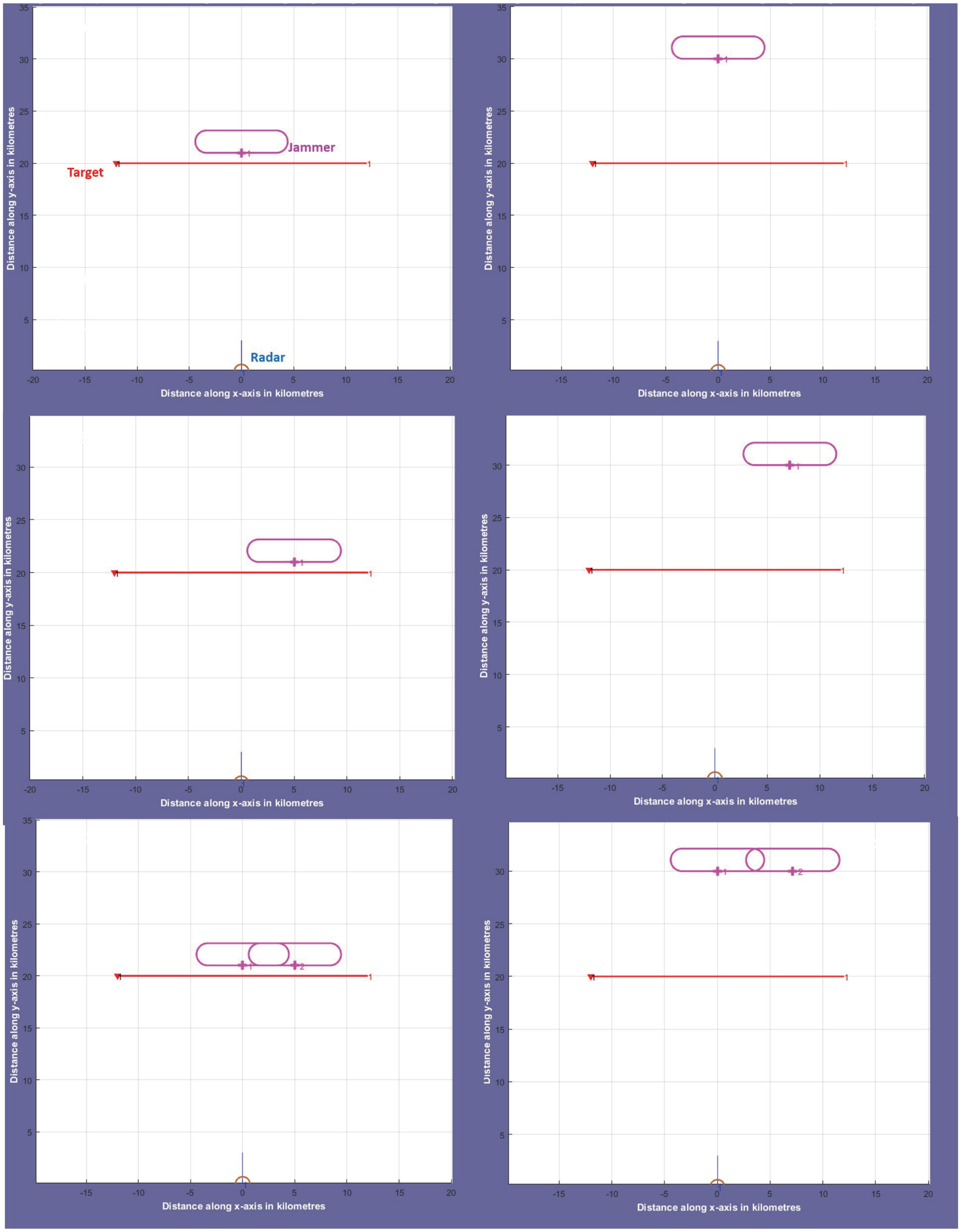

Figure 6: *Jammer and target trajectories for Scenario S1 and S2. (L)Scenario S1 (R) Scenario S2*

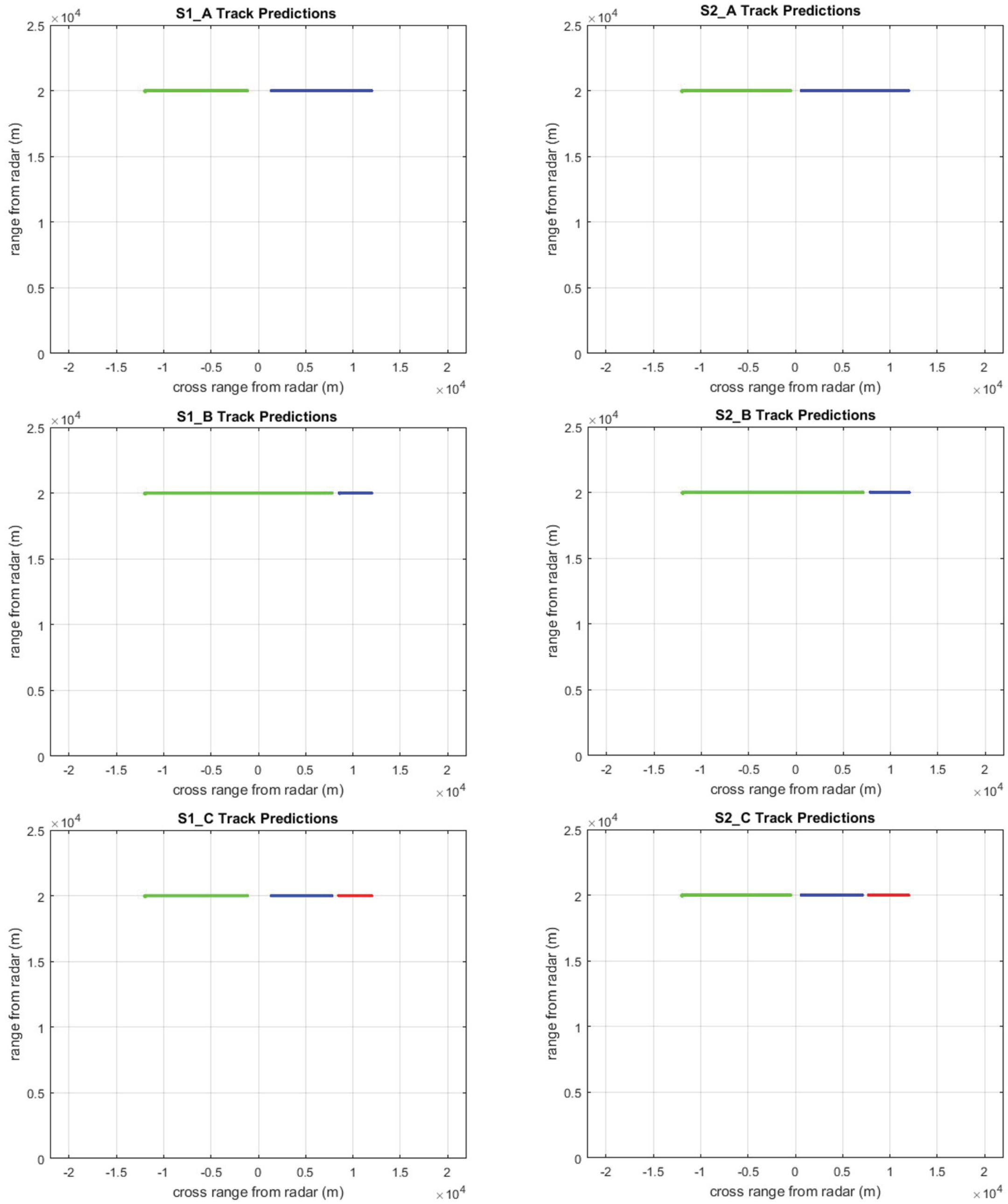

Figure 7: *Target track estimation results for Scenario S1 and S2. (L)Scenario S1 (R) Scenario S2*

Figure 8 and Figure 9 plot the power of the target, jammer and noise for scenario S1 and S2 respectively, they are consistent with the tracking results displayed in Figure 7.

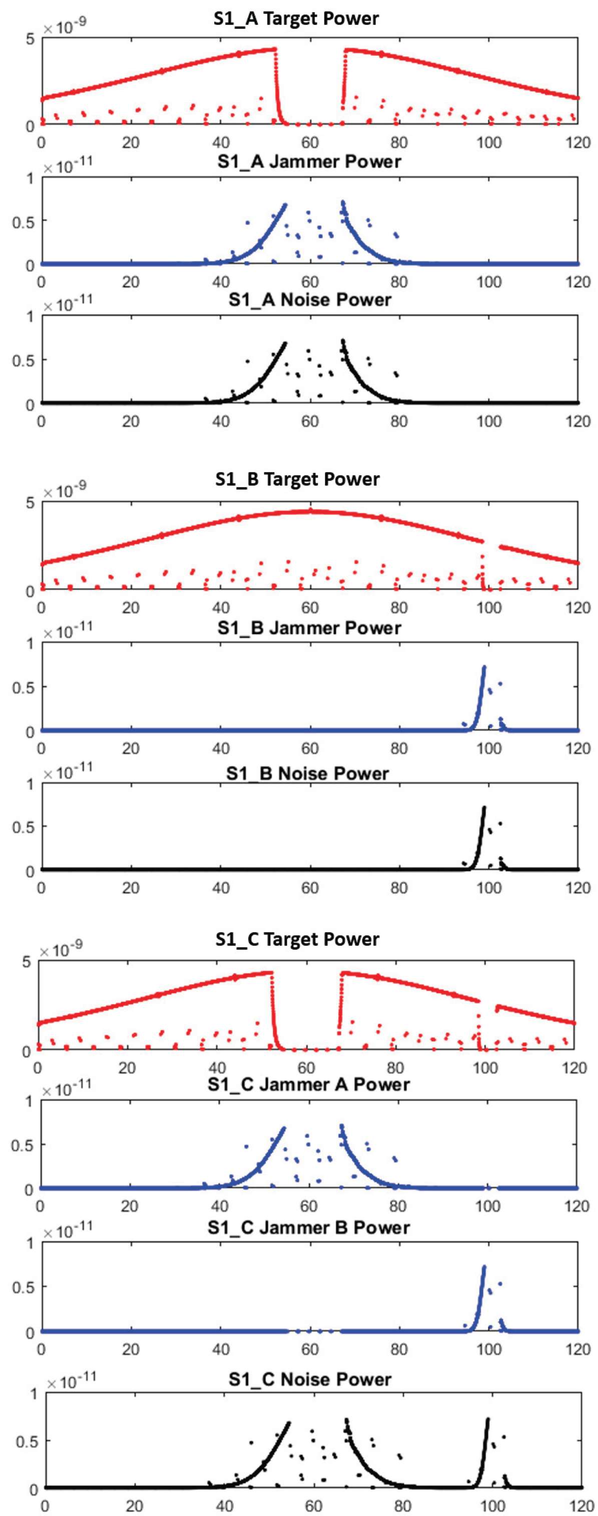

Figure 8: *Scenario S1_A,B,C target and jammer power plot*

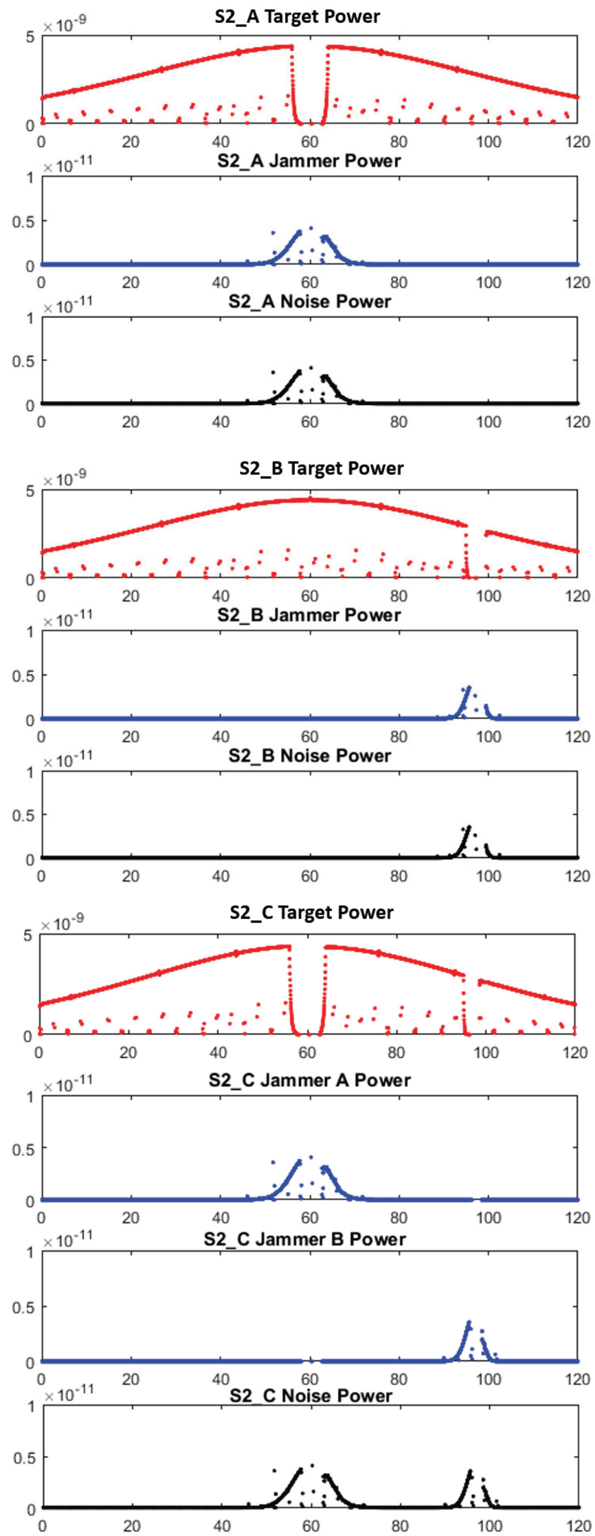

Figure 9: *Scenario S2_A,B,C target and jammer power plot*

2.3 RGPO Function

RGPO is a sophisticated range deception technique. When a target is illuminated by a range-tracking radar, the RGPO technique on the target can pick up the radar pulse, amplify it, and send it back immediately, then the RGPO function will continually emit a series of delayed pulses along with the instantaneous pulse. These deception signals, being stronger than the signals returned from the target, can capture and lock the range gate of the radar so as to pull it off from the actual target. When the range gate is sufficiently removed from it, the target will turn off the deception signal to force the tracking radar to move into a target detection status.

2.3.1 Implementation

Figure 10 explains the range gate pull off technique implemented in Adapt_MFR v3.2.14. In this example, the RGPO technique is activated twice during the target trajectory period: Leg 1 with duration $[t_0^1\ t_k^1]$ and Leg 2 with duration $[t_0^2\ t_k^2]$. The time delays can be controlled so that the false targets, i.e. RGPO legs, can separate from the actual target with linear or quadratic motion. For the linear case, the range of the false target at moment k with respect to the radar is expressed as:

$$R_k^{FT} = R_k^T + v_{po}(t_k - t_0) \tag{6}$$

where R_k^T is the slant range of the actual target at moment k, v_{op} is the rate of pull off, t_0 is the initial reference time of the RGOP leg. For the quadratic case, the range of the false target with respect to the radar is written as:

$$R_k^{FT} = R_k^T + \frac{1}{2}a_{po}(t_k - t_0)^2 \tag{7}$$

where a_{po} is the acceleration of the pull off rate [2].

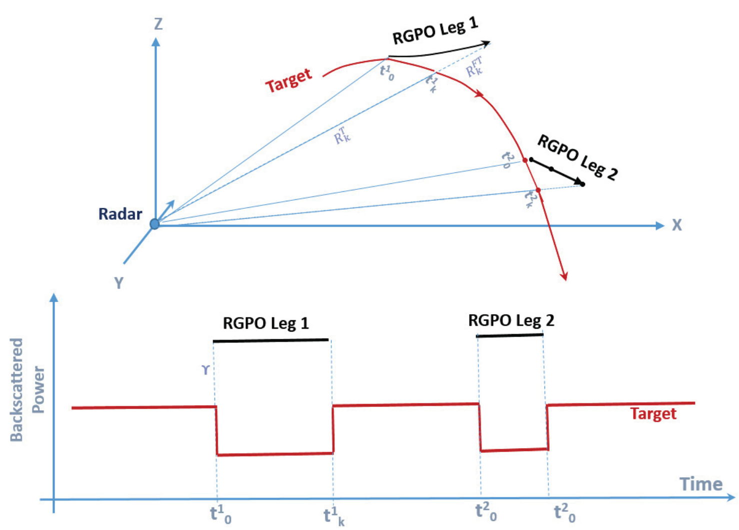

Figure 10: *Range gate pull off technique*

An amplification factor γ is also used to modify the power of actual and false targets as displayed in Figure 10. Once the RGPO is activated, the power of the false target is amplified γ times from the power of the actual target while the power of the actual target is suppressed to the same degree.

Figure 11 displays the RGPO function GUI. For each target given the trajectory time, users can define the number of RGPO legs associated with it, the duration of each leg, the pull off type, rate and amplification factor of the leg. The input parameters from the GUI are saved in a new data structure *missileRGPO* in the parameter file **.mfr* of Adapt_MFR.

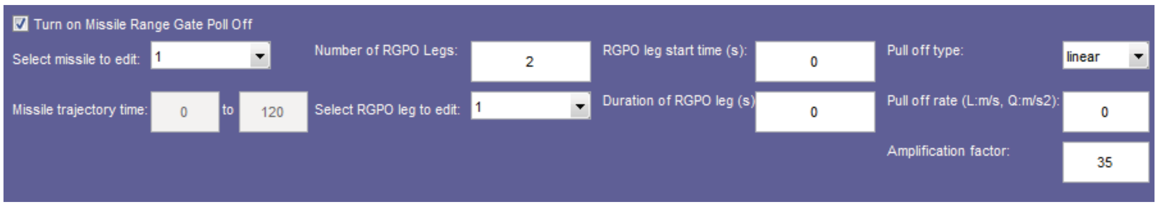

Figure 11: *Range gate pull off GUI*

Table 3 lists the modified and new functions for RGPO routine in Adpat_MFR V3.2.14.

Table 3: *Modifed and new RGPO functions in Adapt_MFR v3.2.14*

Functions Modified:	
adaptmfr_run.m	*Main*
cbMissileParams.m	*GUI*
cbMissileParamsAdd.m	*GUI*
cbViewAzimuth.m	*GUI*
cbSaveParms.m	*GUI*
editUiControl.m	*GUI*
saveMissParams.m	*GUI*
cbJammerParams.m	*GUI*
cbpPlaneView.m	*GUI*
cbConsolidate.m	*GUI*
New Functions:	
RGPO_targets.m	*Main*
RGPO_target_init.m	*Main*
changeMissileRGPOs.m	*GUI*
changeMissileRGPOLegs.m	*GUI*
saveRGPOParams.m	*GUI*

2.3.2 Testing

Scenario S3 was designed to test the RGPO function. The positions of the radars, targets and RGPO legs are displayed in Figure 12. Three targets were included in this experiment. Target 1 flew a simple trajectory remaining at a constant altitude of 3050 m. The RGPO was not activated for this target. Target 2 and 3 are highly maneuvering targets with complex trajectories. Target 2 remained at the same altitude as Target 1 with its speed varying from 457 m/s to 206 m/s during the simulation. Three RGPO legs with 20 second duration were generated for this target. The speed of Target 3 varied from 78 m/s to 342 m/s and the trajectory climbed from 2290 m to 4570 m in altitude in 185 seconds, and two RGPO legs were generated by Target 2. Two radars were used in this experiment to evaluate the impact of distance between target and radar. Target 2 and 3 were closer to both radars than Target 1, which is located more than 90 km away from both radars.

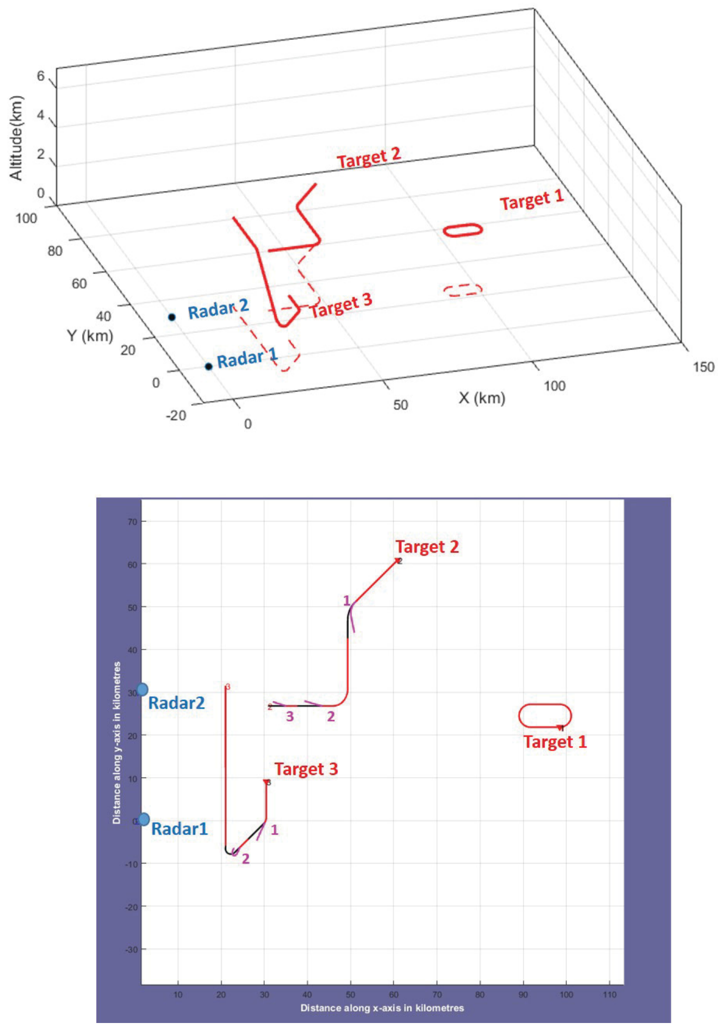

Figure 12: *Target and RGPO trajectories for Scenario S3. (U) 3D view (D) Topview*

Four sub-scenarios were designed in S3 to investigate the effect of the RGPO pull off rate and amplification factors on the radar performance. The RGPO parameters for Target 2 (T2) and Target 3 (T3) used by each sub-scenario are listed in Table 4. In each sub-scenario, only RGPO Leg 1 of T2 were changed, the other RGOP legs used the same parameters as Scenario S3_A.

Table 4: *RGPO leg Parameters for Scenario S3*

Scenario S3_A					
	T2 Leg1	T2 Leg2	T2 Leg3	T3 Leg1	T3 Leg2
Start time:	30	100	130	35	65
Duration:	20	20	20	20	20
Pull off type:	linear	linear	linear	linear	linear
Pull off rate:	100	100	100	100	100
Amplification:	35	6	6	6	6
Scenario S3_B					
Pull off rate:	100				
Amplification:	150				
Scenario S3_C					
Pull off rate:	50				
Amplification:	150				
Scenario S3_D					
Pull off rate:	50				
Amplification:	300				

Figure 13 shows sub-scenario S3_A track prediction results from Radar 1 and Radar 2 as a baseline. The estimated tracks are displayed as the solid lines and the black dots around the solid lines are radar observations. One can see that in this baseline case all the RGPO legs did not succeed in pulling off the radar from the targets. Both radars can track Target 2 and 3 as well as their RGPO legs continually. As the pull off rate and amplification factor changing the tracking results for Target 2 and its RGPO Leg 1 from both radars changed. To compare the results from each sub-scenario, Figure 14 and Figure 15 show the enlarged view of Target 2 and its RGPO Leg 1 tracking results from both radars. The tracking results for the other RGPO legs are not displayed since they are the same as the results Scenario S3_A.

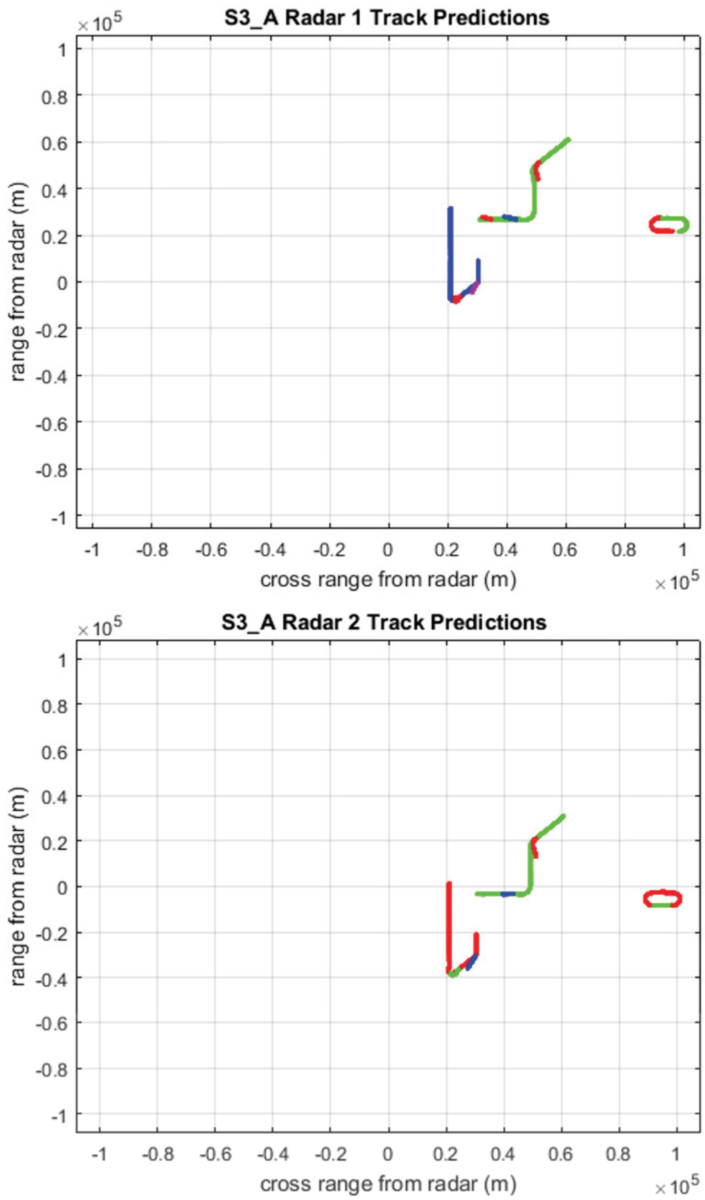

Figure 13: *Radar 1 and 2 track estimation result for sub-scenario S3_A. RGOP Type: linear, Pull off rate: 100m/s, Amplification: 35*

From Scenario S3_A to S3_B in Figure 14, the pull off rate was kept the same and the amplification factor was changed from 35 to 150, one can see that Radar 1 did not track Target 2 during the RGPO Leg 1 period in sub-scenario B since decreased overall target power back at the radar. Both sub-scenarios generated a new track for RGPO Leg 1. From sub-scenario S3_B to S3_C, the amplification factor was not changed but the pull off rate was decreased from 100 m/s to 50 m/s, which means that the fake targets generated by the RGPO would separate more slowly from Target 2. One can see that Radar 1 still doesn't track Target 2 during the RGPO Leg 1 period and also mistakenly combined Target 2 and RGPO Leg 1 trajectories into one track. This means that the tracker's gating algorithm mistakenly believed that the detected signals from RGPO Leg 1 were generated by Target 2. Sub-scenario S3_D generated very similar results as sub-scenario S3_C, which leads to the conclusion that further increasing the amplification factor would not change the results.

The tracking results for Target 2 and its RGPO Leg 1 from Radar 2 are displayed in Figure 15. As shown in Figure 12, Radar 2 is closer to Target 2 than Radar 1 and, in this case, Radar 2 could track Target 2 and its RGPO Leg 1 in sub-scenario S3_A, B and C. The RGPO technique only affects the tracking performance in sub-scenario S3_D where the amplification factor was increased to 300 and the pull off rate decreased to 50 m/s.

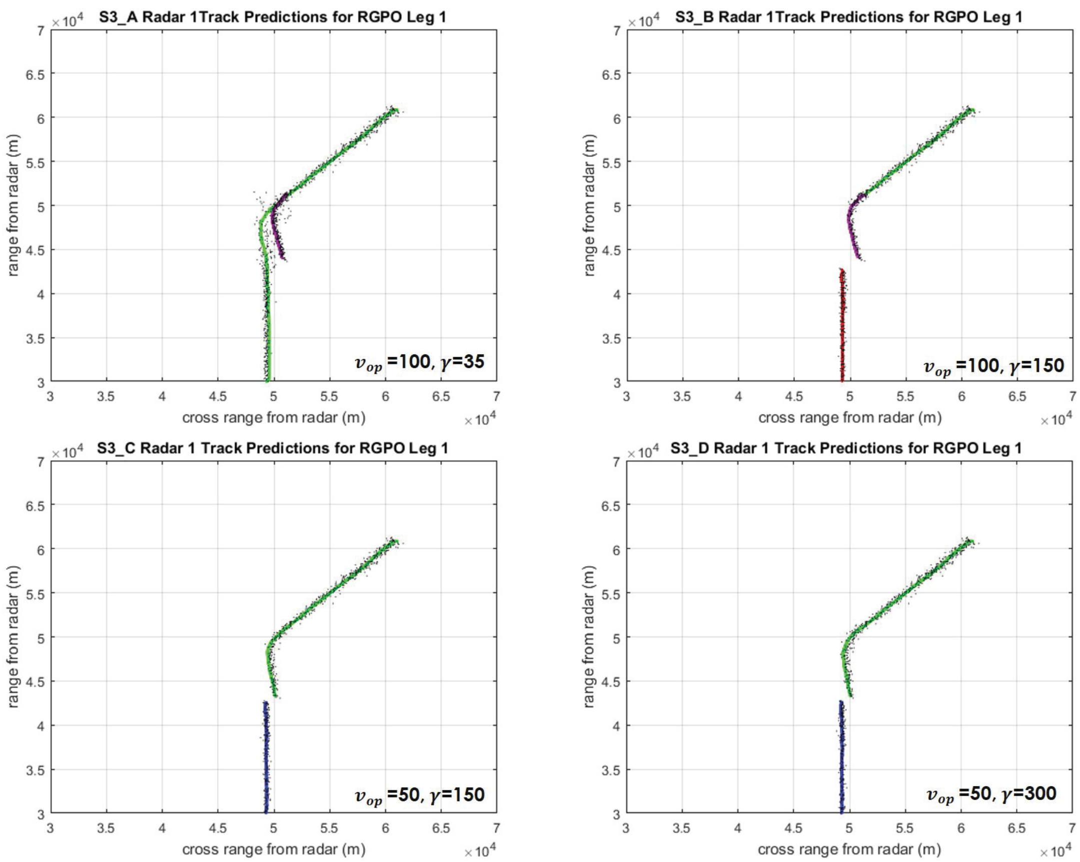

Figure 14: *Target 2 and its RGPO Leg 1 track estimation from Radar 1*

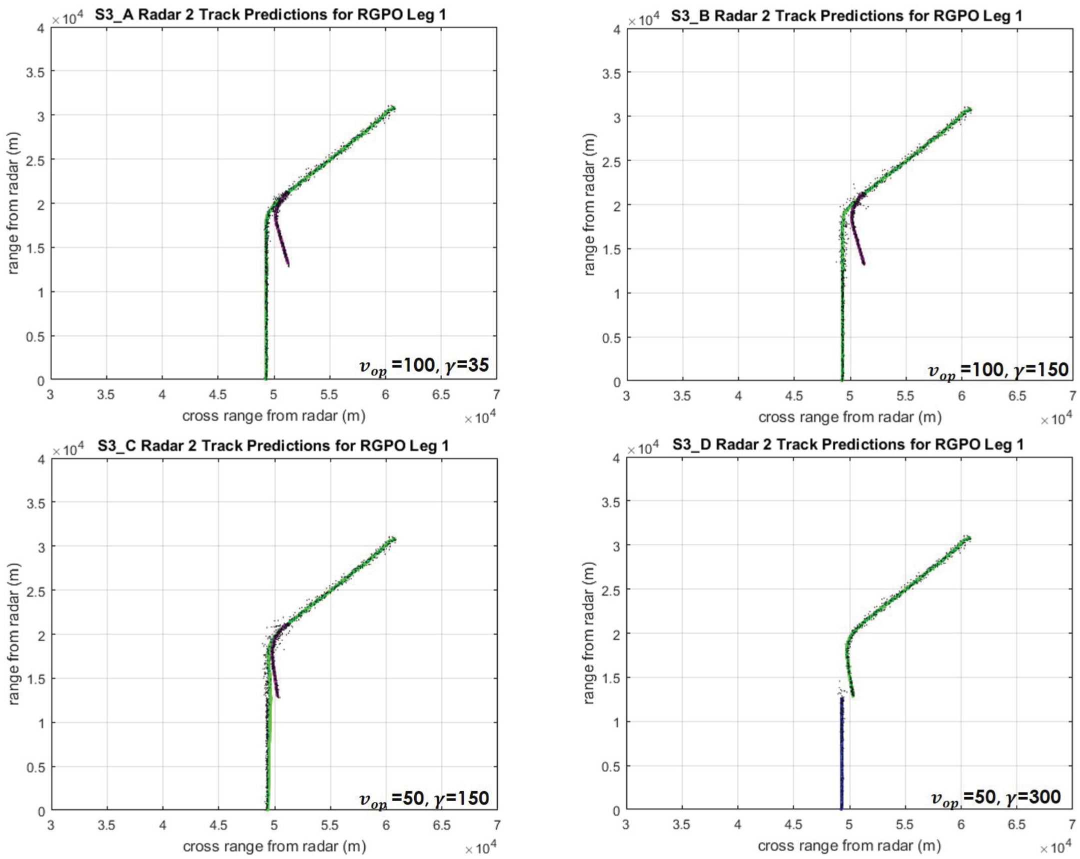

Figure 15: *Target 2 and its RGPO Leg 1 track estimation from Radar 2*

3 Evaluation of Adapt_MFR Target Tracking Performance Against ECM

Scenario S4 was designed to evaluate radar detection and tracking performance against ECM given highly maneuvered targets and FA using Adapt_MFR. Seven sub-scenarios were designed and the complexity of each sub-scenario was increased from sub-scenario A to G. The radar system and ECM components increase in complexity and include a number of radars in the network. Parameters such as FA, RGPO, jammer, beam scheduling strategy (adaptive/non-adaptive), and the gate size were varied in these scenarios.

Three metrics, surveillance frame time, track completeness and track occupancy, were calculated[3] based on the results from each scenario. Radar performance and effectiveness can be evaluated by comparing these metrics and the track estimation results for each sub-scenario.

3.1 Experimental Scenarios

Table 5 sumarizes the complexity of each sub-scenario. The same targets as in Scenario S3_A were used in this experiment, the same FA rate $(6x10^{-4})$ was used for detection, tracking and confirmation beams from sub-scenario S4_B to G, and the RGPO legs on Target 2 and Target 3 were activated from sub-scenario S4_C to G. The topview for target, RGPO leg and jammer trajectories as well as radar locations are displayed in Figure 16. The jammer was generated using the parameters listed in Table 1.

Table 5: *Sub-scenario complexity in Scenario S4*

	S4_A	S4_B	S4_C	S4_D	S4_E	S4_F	S4_G
Radar 1 at [0,0] km	√	√	√	√	√	√	√
Three targets km	√	√	√	√	√	√	√
FA km		√	√	√	√	√	√
RGPO			√	√	√	√	√
Jammer				√	√	√	√
Radar 2 at [0,30] km					√	√	√
Adaptive tracking						√	√
Gate size	16	16	16	16	16	16	8

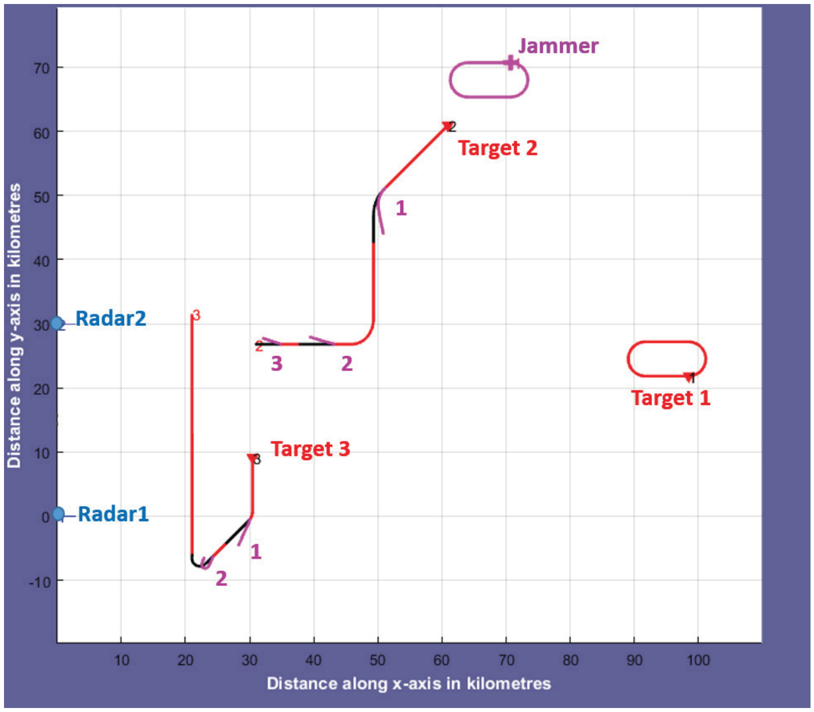

Figure 16: *Radar, target, RGPO and Jammer layout in Scenario 4*

3.2 Tracking Metrics

Surveillance Frame Time

The surveillance frame time of a radar system is the time between surveillance frames in a given region of space. To start a frame, a detection beam starts from the initial position and scans the given region in azimuth and elevation directions. To start, the detection beam scans from first to last position on the first elevation line, when finished, the detection beam moves to the next elevation line and scans from first to last azimuth position again, the azimuth direction scan will be repeated until the detection beam has scanned all defined elevation lines. Track and confirmation beams could also be scheduled in a frame if targets are detected and tracked, the survillance frame time includes:

$$\textit{frame time} = \textit{total time of track} + \textit{total time of confirmation} + \textit{total time of detection} \tag{8}$$

Surveillance frame time can be used to evaluate a radar's efficiency. Longer frame time means longer intervals between each complete surveillance scan over the region so that a target could first be detected with longer delay after it enters the radar coverage.

Track Completeness

A target could exist within the nominal radar coverage but it is not detected by the radar since the radar is not scheduled to look at this target. The track completeness metric is introduced to evaluate radar efficiency on tracking a target. The track completeness of a target is defined by:

$$\textit{track completeness} = \frac{\textit{total time interval over which any track number is assigned to target}}{\textit{total time that target is in the defined radar coverage area}} \quad (9)$$

Track Occupancy

Track occupancy is a fundamental characteristic of all radar systems, it expresses the fraction of available time that the radar is either transmitting or receiving the returns from targets, and defined by:

$$\textit{track occupancy} = \frac{\textit{track time}}{\textit{surveillance frame time}} \quad (10)$$

3.3 Tracking and Metrics Results

The tracking result of each sub-scenario from Radar 1 are displayed in Figure 17 and Figure 18, and the frame time, track completeness and occupancy are displayed in Figure 19. The target index from 1 to 8 in the Track Completeness plot corresponds to Target 1, 2, 3, RGPO Leg 1, 2, 3 of Target 2 and RGPO Leg 1 and 2 of Target 3 respectively.

Comparing the tracking results displayed in Figure 17 and Figure 18, one can see that sub-scenario S4_A, B and C generated similar results. Radar 1 was able to detect and track targets in these cases even when FA and RGPO legs were added in the simulations. However Radar 1 failed to track Target 2 at the beginning of its trajectory when the jammer was added to the simulation in sub-scenario S4_D.

Though similar tracking results were observed for sub-scenario S4_A, B and C, one can see that FA and ECM did affect Radar 1's frame time and track occupancy metrics as plotted in Figure 19. The frame time of sub-scenario S4_B and S4_C are longer than S4_A, and their track occupancies are less than S4_A, this occurred because Radar 1 spent more time on detection and tracking FAs and RGPO legs in the former two sub-scenarios. One can also see that the track completeness of Target 2 in S4_D is lower than the track completeness of this target in sub-scenario S4_A, B and C because of the jamming effect at the beginning of Target 2's trajectory.

Radar 2 was added to the simulation from sub-scenario S4_E to G. However, sub-scenarios S4_E and S4_D have the same complexity since each radar works independently in sub-scenario S4_E, as a result, the tracking result and the metrics of sub-sceario S4_D and E are similar.

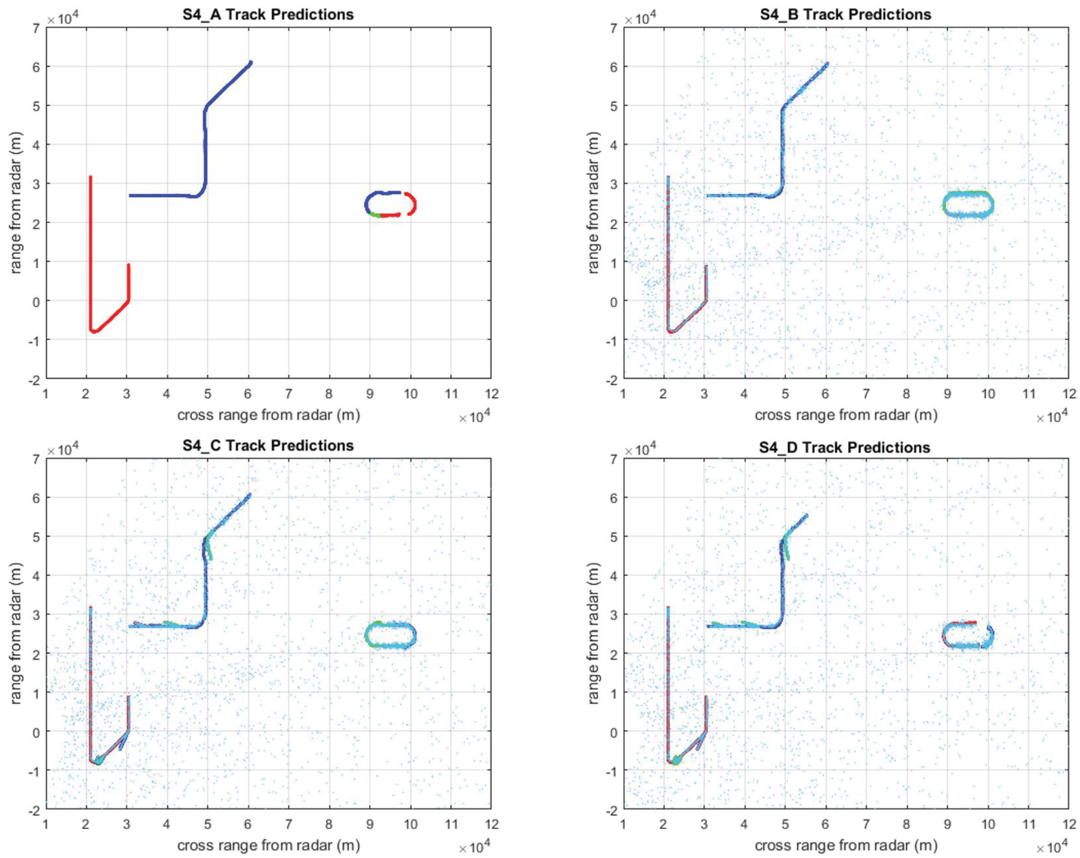

Figure 17: *Scenario S4_A, B, C and D track estimation from Radar 1*

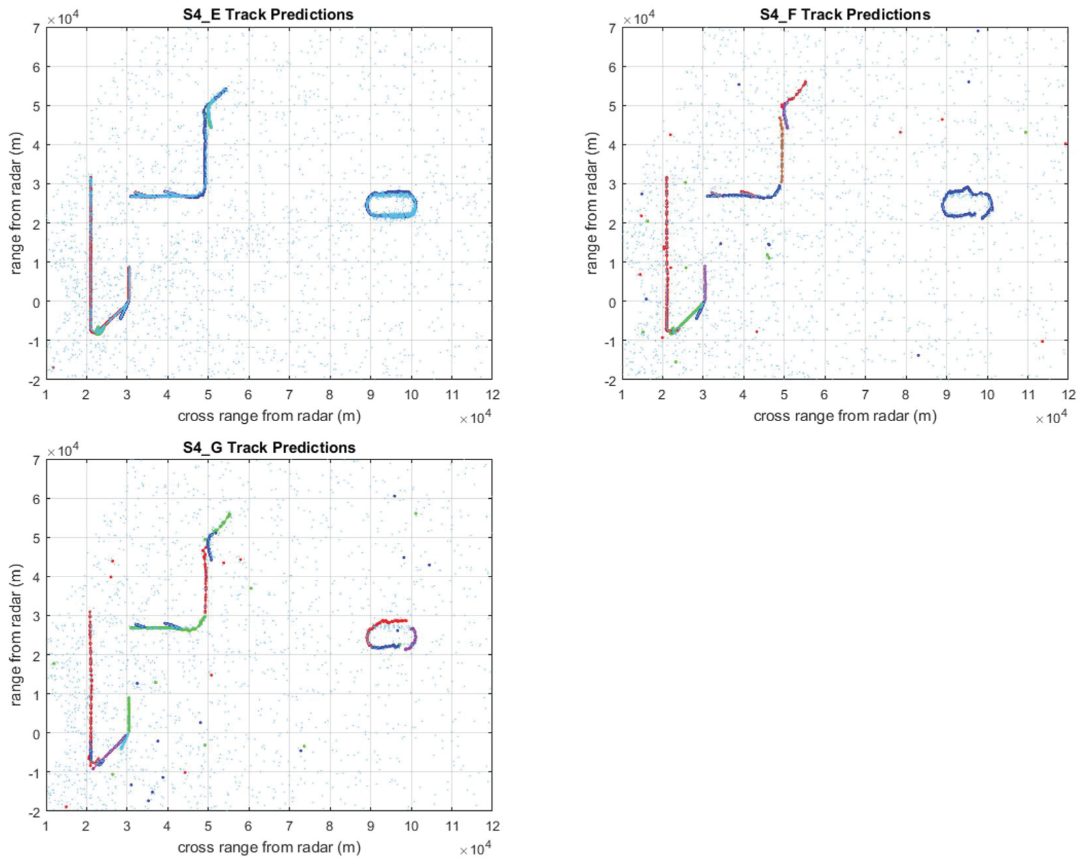

Figure 18: *Scenario S4_E, F and G track estimation from Radar 1*

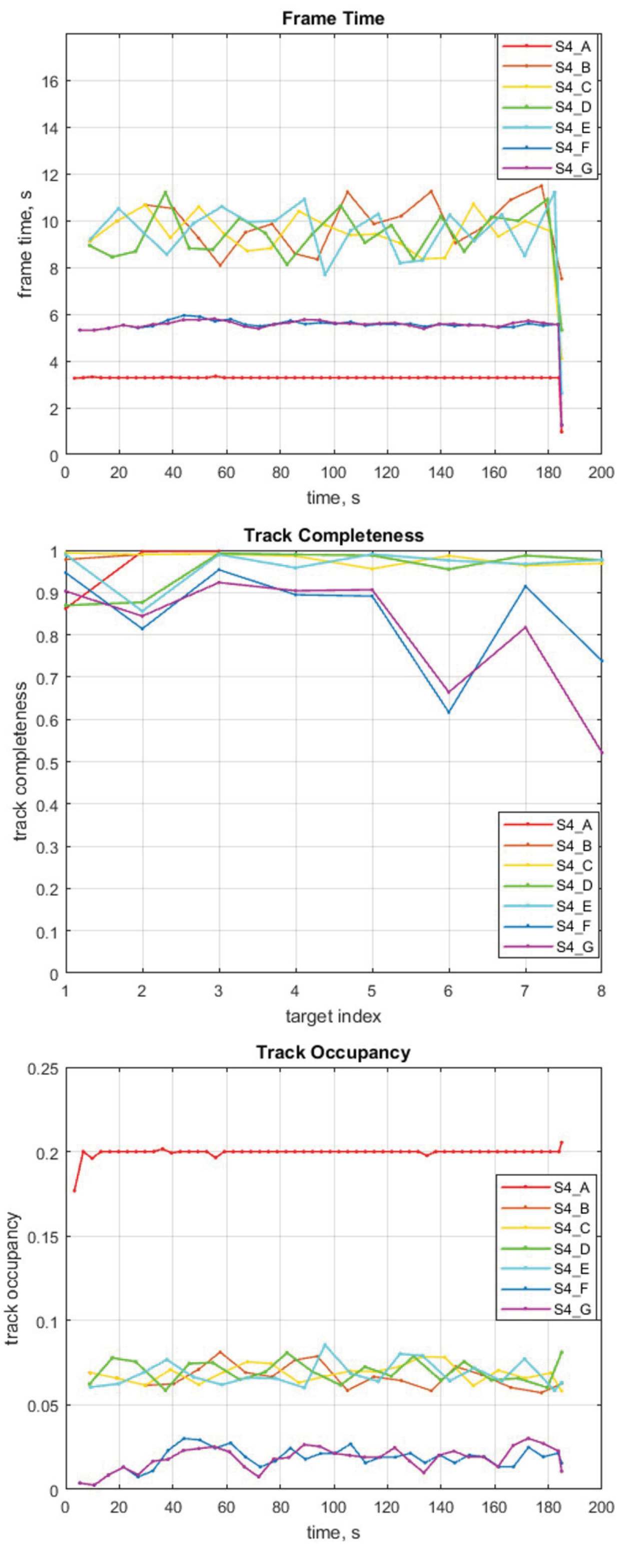

Figure 19: *Scenario S4 frame time, track completeness and occupancy.*

Compared to all non-adaptive sub-scenarios, the two adaptive ones generated worse tracking results when considering track completeness as displayed in Figure 19. One can see that Radar 1 cannot maintain Target 2's and Target 3's tracks every time when the targets made highly maneuvering turns regardless RGPO leg activations (see Figure 18) in these two sub-scenarios.

However, the two adaptive sub-scenarios have the lowest track occupancies compared to all the non-adaptive cases and they also used less frame time than sub-scenario S4_B, C, D and E given the same FA environment. This means that Radar 1 used less percentage of its frame time for tracking and more percentage for detection compared to non-adaptive cases, and Radar 1 also scanned the region more efficiently by using less frame time in the adaptive cases.

No significant differences were observed from metric plots between the two adaptive sub-scenarios. The frame time and track occupancy are very close most of the time. However, sub-scenario S4_G (smaller gate size) performed worse in tracking Target 3 at its last turning position compared to sub-scnario S4_F. Radar 1 tracking results for Target 3 for both sub-scenarios are displayed in Figure 20, one can see that Radar 1 can track Target 3's trajectory more precisely and with less interruptions in sub-scenario S4_F (left). The smaller gate size was thought to be more vulnerable to the FA effect.

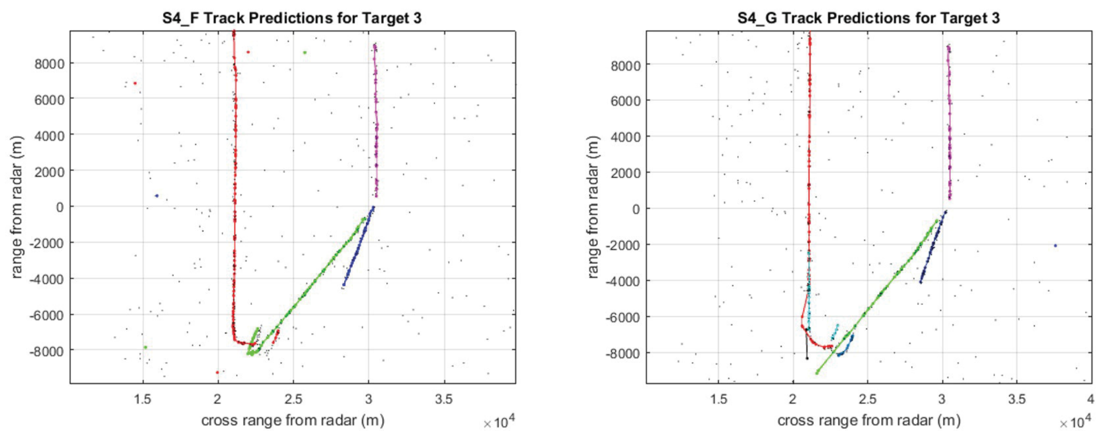

Figure 20: *Scenario S4_F and G Target 3 track estimations from Radar 1. (L) Gate size:16. (R) Gate size: 8.*

4 Discussions and Conclusions

This report summarizes the work done under Task 2 of contract W7714-176210/001/IPS. This work includes the design and implementation of ECM techniques for the Adpat_MFR simulator and evaluation of Adapt_MFR's detection and tracking performance against ECMs given different system setups such as signal or multiple radars, FA, gate size, and beam scheduling technique. The implemented ECMs include RGPO on the target and standoff jamming broadcasting narrow-band noise or white noise covering a specified bandwidth. The existing FA routine in Adapt_MFR has also been modified by adding FAs to the simulation from detection beams.

Two types of standoff jamming techniques have been implemented in this task: spot and barrage jamming. A spot type jammer can jam one frequency while a barrage jammer spreads energy over a wide frequency spectrum. Jamming routine test results showed that given appropriate jamming power and distance between them, a jammer can effectively submerge a target by transmitting interfere noise to the radar direction.

Different from standoff jamming where a jammer is physically separated from its friendly asset, the deceptive RGPO technique is attached to and operated by the target as implemented in this task. The analysis of the RGPO routine test results showed that the RGPO can largely impact radar detection and tracking given appropriate pull off rate and amplification factor. RGPO could either mislead the radar to a wrong track or break a real target track and make the target invisible to the radar. In both cases, the radar will lose the full awareness to the target during the RGPO leg period.

The performance analysis using a set of increasingly complex scenarios showed that the radar effectiveness can be affected by FA, ECM and track scheduling techniques. The FA and ECMs can increase radar frame time and decrease track occupancy, however, they may not affect the track completeness. The track completeness was found to be more affected by track scheduling methods. The adaptive track scheduling can improve radar frame time and track occupancy at the cost of track completeness, therefore it is more suitable for detecting and tracking larger quantities of targets, as more radar time can be assigned for target detections and new track initiations.

5 References

1. Electronic Countermeasure (ECM), Blog at WordPress.com, March 29, 2016.

2. Blair, W. D., G. A. Watson, T. Kirubarajan, and Y. Bar-Shalom. ”Benchmark for radar allocation and tracking in ECM.” IEEE Transactions on Aerospace and Electronic Systems 34, no. 4 (1998): 1097-1114.

3. Tracking metrics for the evaluation of radar scheduling, TTCP Technical Report TR-SEN-05-2007, May 2008

6 List of symbols/abbreviations/acronyms

Adapt_MFR	Adaptive Multifunction Radar
DRDC	Defence Research & Development Canada
ECM	Electronic Counter Measures
FA	False Alarm
PFA	Probability of False Alarm
PRF	Pulse Repetition Frequency
PW	Pulsewidth
RGPO	Range Gate Pull Off

DOCUMENT CONTROL DATA

*Security markings for the title, authors, abstract and keywords must be entered when the document is sensitive

1. ORIGINATOR (Name and address of the organization preparing the document. A DRDC Centre sponsoring a contractor's report, or tasking agency, is entered in Section 8.) C-CORE 4043 Carling Ave. Suite 202 Ottawa (Ontario) K2K 2A4 Canada	2a. SECURITY MARKING (Overall security marking of the document including special supplemental markings if applicable.) CAN UNCLASSIFIED 2b. CONTROLLED GOODS NON-CONTROLLED GOODS DMC A

3. TITLE (The document title and sub-title as indicated on the title page.)

Simulation of Radar Detection and Target Tracking Against Electronic Counter Measures (ECM) Using Adaptive Multifunction Radar (Adapt_MFR) v3.2.14—Final Contract Report

4. AUTHORS (Last name, followed by initials – ranks, titles, etc., not to be used)

Yue, B.

5. DATE OF PUBLICATION (Month and year of publication of document.)	6a. NO. OF PAGES (Total pages, including Annexes, excluding DCD, covering and verso pages.)	6b. NO. OF REFS (Total references cited.)
June 2018	35	5

7. DOCUMENT CATEGORY (e.g., Scientific Report, Contract Report, Scientific Letter.)

Contract Report

8. SPONSORING CENTRE (The name and address of the department project office or laboratory sponsoring the research and development.)

Corporate Office
ADM(S&T) / DRDC Corporate
NDHQ (Carling), 60 Moodie Drive, Building 7
Ottawa, Ontario K1A 0K2
Canada

9a. PROJECT OR GRANT NO. (If appropriate, the applicable research and development project or grant number under which the document was written. Please specify whether project or grant.)	9b. CONTRACT NO. (If appropriate, the applicable number under which the document was written.)
01bd - Future Radar Applications For The Above Water Battlespace	W7714-176210/001/IPS

10a. DRDC PUBLICATION NUMBER (The official document number by which the document is identified by the originating activity. This number must be unique to this document.)	10b. OTHER DOCUMENT NO(s). (Any other numbers which may be assigned this document either by the originator or by the sponsor.)
DRDC-RDDC-2018-C163	Task 2

11a. FUTURE DISTRIBUTION WITHIN CANADA (Approval for further dissemination of the document. Security classification must also be considered.)

Public release

11b. FUTURE DISTRIBUTION OUTSIDE CANADA (Approval for further dissemination of the document. Security classification must also be considered.)

12. KEYWORDS, DESCRIPTORS or IDENTIFIERS (Use semi-colon as a delimiter.)

Multifunction phased array radar; Detection and Target Tracking; ECM (Electronic Countermeasures)

13. ABSTRACT/RÉSUMÉ (When available in the document, the French version of the abstract must be included here.)

This report summarizes the work done under Task 2 of contract W7714-176210/001/IPS. This work includes design and implementation of Electronic Counter Measures (ECM) techniques for the Adaptive Multi-Function Radar (Adpat MFR) simulator and evaluation of Adapt MFR's detection and tracking performance against ECMs given different system setups including single or multiple radar scenarios, varied false alarm rates (FA), tracker gate size, and beam scheduling technique. The implemented ECMs include range gate pull off (RGPO) on the target, and standoff jamming broadcasting narrow-band noise or white noise covering a specified bandwidth. The existing FA routine in Adapt MFR has also been modified by adding FAs to the system on all scans, including detection scans.

Le présent rapport résume les travaux réalisés dans le cadre de la tâche 2 du contrat W7714-176210/001/IPS. Les travaux englobent la conception et la mise en œuvre de techniques de contre-mesures électroniques (CME) pour le simulateur de radar adaptatif multifonction (RAM) et l'évaluation de ses performances de détection et de poursuite en fonction des CME selon diverses configurations de systèmes, y compris pour des scénarios à un ou plusieurs radars, à divers taux de fausses alarmes (FA), selon la taille de la porte de la balise et la technique de programmation des faisceaux. Les CME en place comprennent le déréglage des portes de distance (RGPO) de la cible, ainsi que le brouillage à distance de sécurité diffusant du bruit à bande étroite ou du bruit blanc couvrant une largeur de bande donnée. La procédure actuelle de FA du RAM a aussi été modifiée par l'ajout de FA au système pour tous les balayages, dont les balayages de détection.